ELSEVIER

15 April 2002

Physics Letters A 296 (2002) 109–116

PHYSICS LETTERS A

www.elsevier.com/locate/pla

Intense laser pulse amplification using Raman backscatter in plasma channels ☆

P. Mardahl [a,*], H.J. Lee [a], G. Penn [a], J.S. Wurtele [a], N.J. Fisch [b]

[a] *University of California, Berkeley and Lawrence Berkeley Laboratory, Berkeley, CA 94720-7300, USA*

[b] *Princeton Plasma Physics Laboratory, Princeton, NJ, USA*

Received 22 January 2002; received in revised form 22 January 2002; accepted 5 March 2002

Communicated by F. Porcelli

Abstract

It has been proposed that the Raman backscatter interaction in a plasma can be used to amplify ultra-intense laser pulses. To accomplish this, energy is transferred from a long drive pulse at frequency ω_{pump} to an intense seed pulse at frequency ω_{seed}, with a Langmuir plasma wave at frequency w_{p} mediating the transfer; the frequencies are chosen to satisfy the resonant condition $\omega_{\text{p}} = \omega_{\text{pump}} - \omega_{\text{seed}}$. Diffraction of the pulses limits the interaction length in a uniform plasma, and hence the energy transfer between the pulses. However in a parabolic plasma density channel it is shown, through two-dimensional particle-in-cell simulations, that such a plasma channel can be used to guide both the amplified and drive pulses over an interaction distance much greater than a diffraction length. The seed pulse is amplified by a factor of more than 200 in energy for pulses whose widths are matched to the channel size, and achieve a peak intensity of more than 6×10^{17} W/cm^2. Unmatched pump pulses are seen to generate much smaller gain.

PACS: 52.40.Nk; 52.65.-y

Keywords: Laser; Plasma; Raman backscatter

1. Introduction

Backward Raman amplification has been studied in liquids, gases and plasmas, with a view towards construction of backward wave oscillators, pulse compression and pulse amplification [1–4]. The Raman backscatter pulse-compressor has attracted attention recently because of the observation that, at high power, pulse compression in plasmas can operate in the so-called π-pulse regime, where the pulse length compresses as it amplifies [5]. Regimes were identified where the compression occurs fast enough to avoid deleterious instabilities. The resulting amplifiers are capable, in principle, of unfocused output laser intensity on the order of 10^{17} W/cm^2. Recent experiments support the Raman backscattering amplification effect in plasma [6].

Before the development of chirped pulse amplification (CPA) in the mid-80s, laser intensities were limited to GW/cm^2 due to distortions related to nonlin-

☆ Work supported by DARPA.

* Corresponding author.
E-mail address: peterm@eecs.berkeley.edu (P. Mardahl).

0375-9601/02/$ – see front matter
PII: S0375-9601(02)00194-9

ear propagation in conventional amplifiers. Currently, CPA reaches TW/cm^2 intensities without focusing by longitudinal compression of long laser pulses after amplification. The gratings needed to stretch and compress the laser pulses become quite large and expensive in order to reach intensities beyond the petawatt per cm^2 range, and are subject to damage by the laser pulse. In addition, the amplification must be precisely linear.

Because of these issues with CPA amplifiers, it is natural to consider plasma-based systems for the formation and manipulation of ultra-high intensity lasers. The amplification of Raman backscatter is shown schematically in Fig. 1. In this process [5], energy is transferred from a low-intensity long pulse to a high-intensity short pulse using a plasma resonance. Particularly promising is the recent suggestion that the Raman backscatter interaction in plasma may avoid unwanted instabilities not only of the short pulse, but also of the pump laser, during the time the short pulse is amplified to extremely intense powers [7,8].

These considerations [7,8] of the Raman backscattering effect at high powers assumed that the amplification takes place in an infinite homogeneous plasma. That model would be valid only if the plasma amplifier is much shorter than a Rayleigh diffraction length ($Z_R \equiv \pi W_0^2/\lambda$, with W_0 the minimum spot size). In the limit that the spot size is small, in order to achieve high power density without the expense of high total power, it will be important to propagate the lasers in a plasma channel of small diameter, as has been done experimentally in a capillary plasma discharge [9]. For 1 μ wavelength radiation amplified over a cm length of plasma, this requirement implies restriction to a spot size of much less than 100 μ.

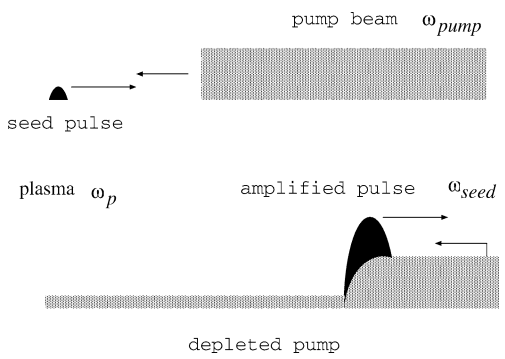

Fig. 1. Schematic of Raman backscatter interaction; $\omega_{\text{pump}} - \omega_{\text{seed}} = \omega_{\text{p}}$.

The present study offers preliminary examination of the physical effects that occur during such amplification in a plasma channel. The main points of interest here are the theoretical and simulated efficiencies of such a process, the mode structure of the output beam, and the achievable intensity of the laser at its focus.

The Letter is organized as follows: In Section 2, we describe the 2d PIC simulation that we employed for the study. In Section 3.1, we present the results simulations in a homogeneous plasma. In Section 3.2, we present results of simulations in parabolic plasma channels. In Section 4 we present our conclusions.

2. XOOPIC simulation

The XOOPIC [10] code is used to simulate the counter-propagating laser pulses in plasma in a two-dimensional Cartesian domain; the two laser beams being simulated are finite in length in the direction of propagation and in one transverse dimension, but infinite and uniform in the third dimension. XOOPIC uses a particle-in-cell algorithm with a finite difference time domain field solver. This is a first-principles model which self-consistently solves the Lorentz force equation for the particles and solves Maxwell's equations for the fields.

A few modifications of the XOOPIC code were required to enable the simulation of the Raman backscatter pulse amplification (these modifications are discussed in detail in Ref. [11]). The XOOPIC code solves for the total electric and magnetic fields, with no assumptions about the direction of propagation. Obtaining diagnostics of the amplification process requires that the left- and right-propagating waves be separated. This is accomplished by using simple expressions (in MKS units):

$$A_{\text{left}} = \frac{E_y - cB_z}{2}, \qquad A_{\text{right}} = \frac{E_y + cB_z}{2}. \tag{1}$$

The finite difference implementation of these expressions is not exact, because the electric and magnetic fields are not calculated at the same mesh positions. An interpolation scheme that was employed produces an error of less than 1%; that is, launching a wave in one direction yields a diagnostic result that has

less than 1% field signal in the counter-propagating direction.

The interaction takes place over millimeter scale lengths, or 200 to 1000 laser wavelengths, while the growing pulse is only tens of microns in length and the laser wavelengths are of order one micron. A full simulation over such disparate spatial scales is computationally expensive. We use a moving window, in which the only region simulated is approximately 50 microns long. This window contains the growing pulse, which has a length of 5–15 microns, but not the pump pulse, which can be thousands of microns long. This approach greatly reduces the computation time.

Fields and particles are treated in the laboratory frame: the moving window is "moved" simply by shifting all the particles and fields by one mesh pitch Δx every $\Delta x/(c\Delta t)$ timesteps so that the window has speed c. Fields and particle distributions are specified analytically at the leading edge of the window. There are many possible ways to specify the incoming pump pulse and the incoming plasma. In the simplest model (which we did not use) the plasma could be assumed cold and the fields taken as those of a free-space plane wave. More realistically, the fields and the particles should correspond to self-consistent linearized motion from theory. The transverse profile could be a plane wave, a diffracting wave, or a matched guided wave in a channel. For a matched guided wave, the width of the Gaussian laser pulse was chosen to be constant as it propagated down the plasma channel. Particles and fields are discarded at the trailing window boundary: since they are being left behind at speed c they cannot influence the dynamics in the moving frame after falling behind the window. Conducting boundaries were used at the transverse boundaries.

For these simulations, a square numerical mesh was used with a cell size of 0.05 μ. This size resolved the laser wavelengths of interest, which were of the order of 1 μ. Each macroparticle in the simulation represents 10^{10} electrons; the ions are assumed to be immobile on the timescales of interest. The timestep was chosen to be 10^{-16} s, corresponding to roughly 30 timesteps per laser period, and many more per plasma period. The XOOPIC code allows arbitrary initial transverse and longitudinal profiles of the laser pulses to be specified. For these simulations, the seed pulse is always assumed to have an initially Gaussian transverse profile and either a flat-top or a half-sinusoidal longitudinal profile. The phase and group velocity of the seed pulse was typically very near c, and so was well-contained by the moving window. The pump is always longitudinally flat-top on introduction to the system, and has transverse profiles that are either Gaussian or plane wave. The dimensionless vector potential of the laser, defined as $a = eE_{\max}/mc^2\omega$, is typically 0.05 for the pump wave. This intensity is somewhat larger than the wavebreaking point, $a_{\mathrm{br}} \approx 0.25(\omega_{\mathrm{p}}/\omega)^{3/2}$, where the Raman resonance begins to be affected by wavebreaking; this regime is characterized by a single peak in intensity rather than many, as in the π-pulse regime (see the 1-D simulation in Ref. [5]). For all the simulations in this Letter, the frequency of the seed pulse is chosen to be at Raman resonance, $\omega_{\mathrm{seed}} = \omega_{\mathrm{pump}} - \omega_{\mathrm{p}}$, corresponding to peak gain in the weak-pump linear regime.

3. Simulation results

In this section we discuss the main results. Simulations were made to compare the amplification in a homogeneous plasma, where the interaction length is limited by diffraction of the seed pulse, with that in a channel where the guided pulses may interact for many diffraction lengths. The simulations demonstrate that (at least for the idealized approximation that the incoming plasma is cold and the pump wave does not break up as it propagates) the channel can successfully guide both the pump and the seed waves, resulting in enhanced performance over that obtained with parameters where the diffraction limits the interaction length.

Previous simulations have been made with one-dimensional codes [12,13]. Our simulations are the first to report two-dimensional results that include diffraction and plasma channels.

3.1. Amplification in a homogeneous, uniform plasma

Amplification in a homogeneous plasma is the easiest to realize. We have modeled this in XOOPIC by injecting a seed pulse with a 4 μ waist (that is, focus, or minimum spot size) at the plasma entrance. The plasma has a uniform density of $n_0 = 1.0 \times 10^{25}$ m^{-3}, and the Rayleigh length $Z_{\mathrm{R}} \simeq 50$ μ. After the seed pulse travels 36 μ, the moving frame is

initiated and interaction with a counter-propagating plane wave pump pulse begins; this wave is assumed to be a plane wave with dimensionless amplitude $a_0 = 0.047$, shifted up in frequency from the seed pulse by the plasma frequency.

The results of this simulation are shown in Fig. 2. Energy is transferred from the left-going pump pulse to the right-going seed pulse. The seed pulse increases in intensity and expands transversely. Since the incoming pump pulse was modeled as a plane wave, the pump field will have a local RBS coupling whose strength is independent of transverse position. Hence, diffraction will not severely limit the growth. Prior to saturation (end of growth), one expects that the growing mode will diffract until the diffractive (spreading) 'losses' are balanced by the gain. For the simulations reported here, however, the seed pulse reflects off the transverse boundary of the plasma at an interaction length on the order of 200 μ. In Fig. 2 the pulse appears distinctly non-Gaussian due to saturation at the center of the pulse (where the seed was initially larger) occurring before saturation at the wings of the pulse. The undesirable reflections from the wall are clearly visible. The total energy in the pulse, measured in J/m in slab geometry, is plotted as a function of interaction length in Fig. 3. After an initial interval during which the seed pulse enters the plasma, the interaction begins and a roughly exponential growth is observed. The seed pulse grows significantly, approximately a factor of 200 in energy. The peak field grows to a strength of $a_1 = 0.045$, ten times the initial seed strength of $a_1 = 0.0047$. The pulse also shortens somewhat in length. Note that the growth in energy is due to two effects: increase in pulse intensity, and increase in pulse transverse size.

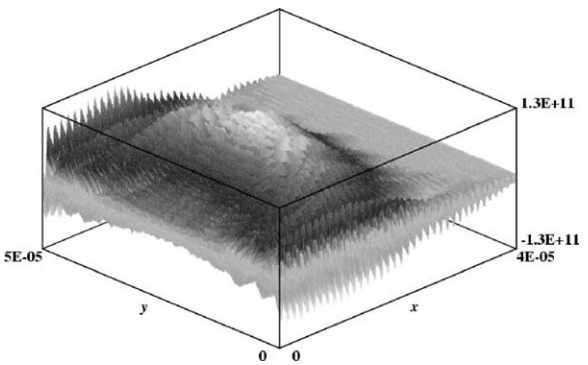

Fig. 2. Wave amplitude in J/m for Gaussian seed pulse is shown after a 220 μ interaction with a planar pump wave. The pump strength was $a_0 = 0.047$ ($E = 1.5 \times 10^{11}$ V/m) and the initial seed strength was $a_1 = 0.0047$. Propagation of the seed pulse, which had an initial transverse spot size of 4 μ, is in the positive x direction, and the seed pulse was at a focus at $x = 0$. The walls parallel to the x-axis have metallic boundary conditions, and the pulse has started to reflect from them. This pulse gained about a factor of 200 in energy and 10 in intensity in 220 μ of interaction.

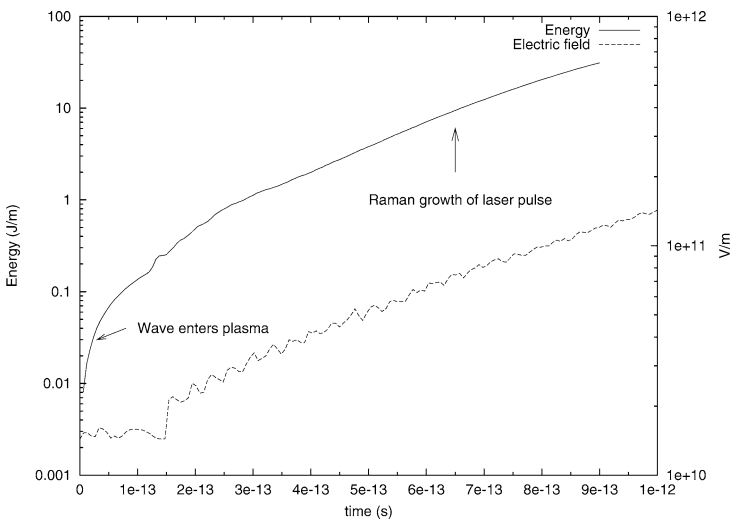

Fig. 3. Energy and peak field amplitude growth of the seed laser pulse. The RBS interaction started at $t = 1.3 \times 10^{-13}$ s. Parameters are the same as for Fig. 2.

A second simulation is performed in which the seed pulse is emitted from the left-hand wall with a focus at $x = 150$ μ, in order to postpone the occurrence of the undesirable reflections from the metal side-walls. Fig. 4 shows the pulse after it has interacted with the plane wave pump for 220 μ without significant interaction with the metal side-walls. The forward focusing delayed the onset of the undesirable reflections off of the metal walls. The energy and amplitude growth of this pulse can be seen in Fig. 5; the pulse has gained a factor of 280 in energy and 10 in peak intensity in 330 μ of interaction.

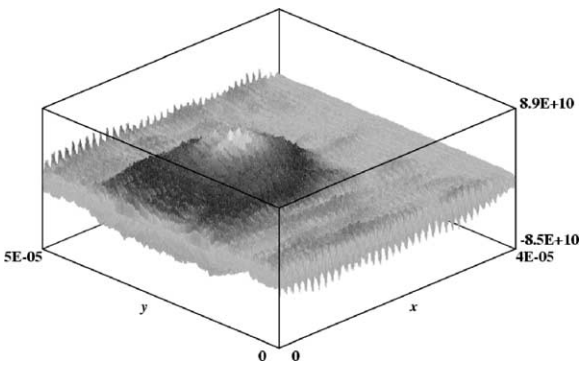

Fig. 4. Amplitude of the seed pulse in V/m after 220 μ of interaction. The growth started at $t = 1.3 \times 10^{-13}$ s. The focus of the seed pulse is at 150 μ and the transverse profile is seen to be better confined than in Fig. 2. This postponed reflections from the walls.

3.2. Enhanced amplification in a parabolic plasma channel

The pump wave in the previous examples was a plane wave. This is unrealistic, since the interaction length was much longer than the diffraction length. In principle one could use a very wide pump wave, so that it appeared planar near the region occupied by the seed. This method is very inefficient since most of the pump energy would not cause growth in the narrower seed pulse.

An attractive solution is to use a plasma channel to guide both the pump and seed pulses. In the first simulation a Gaussian seed pulse interacts with a *plane wave* pump pulse in a channel with a parabolic profile with density $n_0 = 10^{25}$ m^{-3} in the center of the simulation and $n = 4 \times n_0$ on the edges of the simulation. This plasma channel focused the seed pulse sufficiently to allow a much greater interaction length before the seed pulse reached the metal side-walls of the simulation. The transverse expansion of the pulse was not due to diffraction in this case, since the channel has a sufficient density gradient to keep the seed pulse focused. Instead, the pulse amplitude grew transversely with the RBS interaction, resulting in a very non-Gaussian pulse shape, as seen in Fig. 6. Fig. 7 shows the growth in energy of about a factor of 1000 and an increase in peak field intensity of about 44. The initial seed strength was higher in this case, $a_0 = 0.046$, and the initial pulse length was shorter, 15 μ.

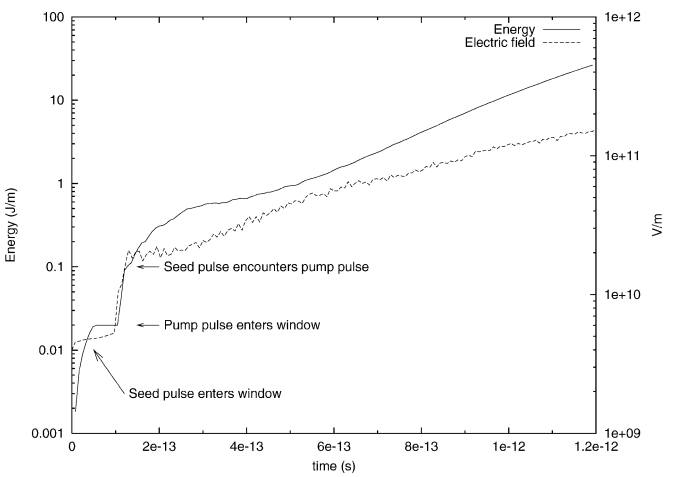

Fig. 5. Energy growth of the seed laser pulse. The kink in the curve near $t = 1.3 \times 10^{-13}$ s to $t = 3 \times 10^{-13}$ s is due to a spurious measurement of the left-going pump pulse as part of the right-going pulse. Exponential growth is observed.

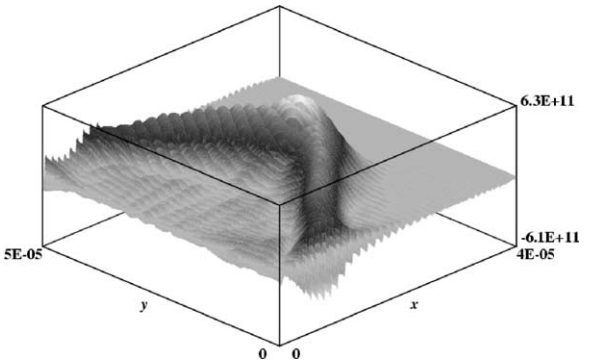

Fig. 6. The seed laser pulse after 344 μ of interaction in a parabolic plasma channel with a counter-propagating plane wave pump.

A more realistic simulation has both the seed and pump pulses matched (shaped) to the channel. An example of this has the pump pulse and the seed pulse both set to an initial waist size of 6 μ for the channel discussed above. Total amplification of the pulse was reduced from the plane wave case because of a reduction in growth rate out in the transverse tails of the seed pulse. In this run, the peak amplitude of the pump was kept at the same value of $a_0 = 0.047$. In some ways, this is not an ideal comparison with an example of a plane wave pump. For example, the energy in the plane wave pump is much higher than that in the guided pump, which is restricted to a 6 μ transverse size by the channel. Propagation appears to be very stable. Fig. 8 shows snapshots of the seed pulse at four times as it propagates down the channel. One can observe that the pulse gradually drops back from the leading edge of the moving window on the right-hand side, which is moving at exactly c, and that the pulse initially broadens longitudinally but then narrows again as it grows. Fig. 9 shows the energy and amplitude growth for this case, which can be seen to begin to level off. The energy grew by a factor of approximately 230 and the peak amplitude by an order of magnitude. Saturation is occurring towards the end of the interaction; at this point the pump depletion is approximately 30%. The initial seed strength was $a_1 = 0.045$.

4. Conclusions

The Raman backscatter interaction has been simulated in plasma channels in a two-dimensional (slab) configuration. The results show first, that there is real gain, and second, that interaction lengths much larger than a diffraction length have been achieved. We have also shown that laser intensities greater than 6×10^{17} W/cm^2 can be achieved.

Although the total laser amplification, measured in power transferred from the pump laser to the seed laser, is somewhat reduced from one-dimensional theory or simulations, this is not the most useful figure of merit for the analysis of these systems. Depending

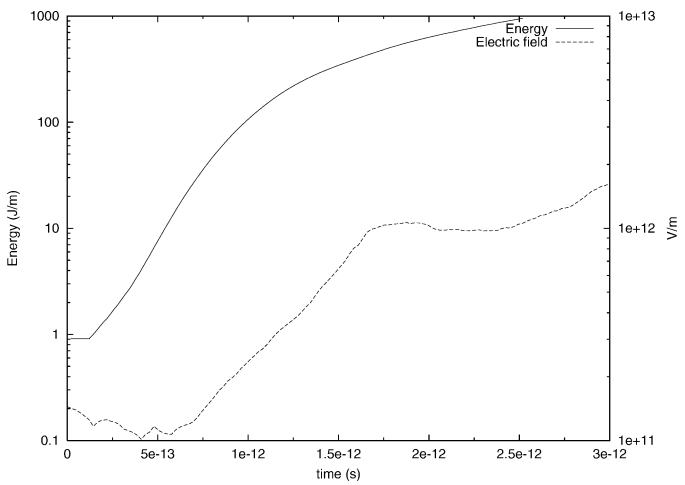

Fig. 7. Energy growth and peak amplitude of the seed laser pulse. Interaction started at $t = 1.3 \times 10^{-13}$ s. The plasma channel prevented the seed pulse from diffracting in y.

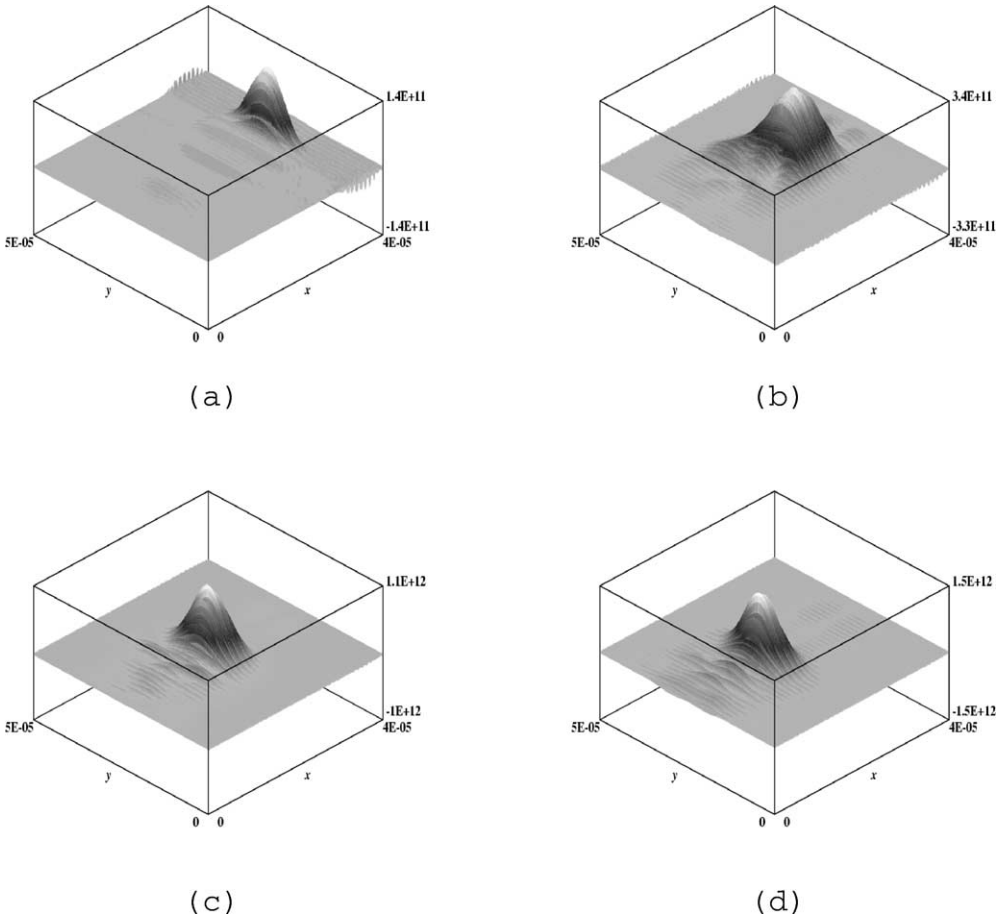

Fig. 8. Snapshots of the seed laser pulse after (a) 10 μ, (b) 330 μ, (c) 730 μ, and (d) 1010 μ of interaction with a counter-propagating Gaussian pump wave. The channel keeps the growing wave focused.

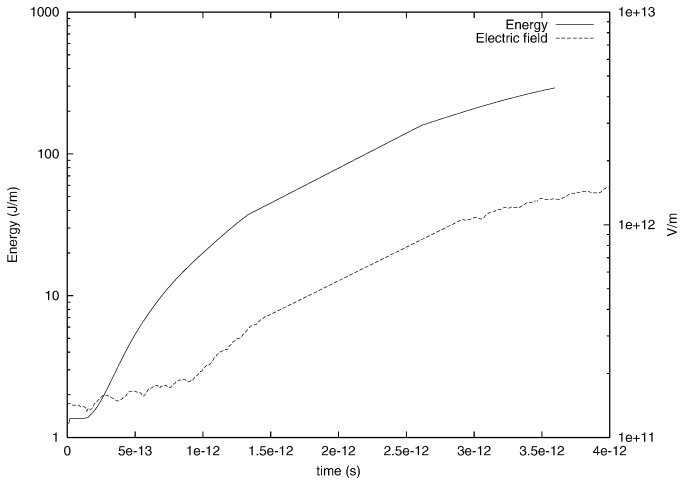

Fig. 9. Energy growth of laser pulse for the parameters of Fig. 8. Both the seed and pump pulses were guided by the plasma channel.

on the purpose to which this method of manipulating lasers will be applied, different figures of merit will have to be considered. Of primary interest are the total power of the pump laser, the peak power of the resultant seed laser, and the efficiency of the energy transfer between the two laser pulses. It is clear that using a plasma channel is better than allowing diffraction of the laser pulses; the cross section and thus total power of the pump laser is much reduced compared to simulations of a uniform plasma which yield a similar amplification. Other alternatives to channel guiding, such as small overmoded waves in metal pipes, remain to be considered.

Some uncertainties arise from the nature of the simulations undertaken so far. In particular, the moving simulation window reduces the tendency of the pump laser to be unstable due to numerical noise; the short window scheme may overcompensate and prevent true instability for long interaction lengths. There are several ideas for controlling this instability in practice [7, 8]. Other issues which have yet to be explored are the effects of mismatch of the pump and seed lasers to the channel, as well as spatial variations of the channel properties, which may reduce the overlap of the pulses or lead to a more complex mode structure. The guiding of the output laser out of the plasma and onto a narrow focus remains to be simulated. In addition, for plasmas generated by the seed pulse laser itself, ionization processes must be properly modeled.

Simulations in a 2d PIC code have yielded results which broadly agree with one-dimensional simulations; diffraction is seen to be an important effect when propagating for many Rayleigh lengths, but plasma channels have been shown to allow very long interaction lengths. We can conclude that at least in a slab configuration, the use of narrow beams in channels offers significant reductions in the total input power required to yield a high-intensity laser pulse, compared to larger beams which could more appropriately be treated as one-dimensional. Future studies will examine cylindrical beams.

These simulations indicate that laser amplification using the Raman backscatter interaction in a plasma channel appears very promising as a means to achieve a high intensity pulse with a moderate total power in the pump. Such a system would enable the construction of nearly table-top scale experiments with peak intensities far above what is currently achieved with CPA amplifiers. With pulse compression occurring over a sufficiently long interaction length, it is possible that a low power input laser could be used without reducing the peak power of the amplified laser pulse.

References

[1] M. Maier, W. Kaiser, J.A. Giordimaine, Phys. Rev. Lett. 17 (1966) 1275.
[2] J.R. Murray, J. Goldhar, D. Eimerl, A. Szoke, IEEE J. Quantum Electron. 15 (5) (1979) 342.
[3] R.D. Milroy, C.E. Capjack, C.R. James, Phys. Fluids 22 (10) (1979) 1922.
[4] J.A. Caird, IEEE J. Quantum Electron. 16 (4) (1980) 489.
[5] V.M. Malkin, G. Shvets, N.J. Fisch, Phys. Rev. Lett. 82 (1999) 4448.
[6] Y. Ping, I. Geltner, N.J. Fisch, G. Shvets, S. Suckewer, Phys. Rev. E 62 (4) (2000) R4532.
[7] V.M. Malkin, G. Shvets, N.J. Fisch, Phys. Rev. Lett. 84 (6) (2000) 1208.
[8] V.M. Malkin, G. Shvets, N.J. Fisch, Phys. Plasmas 7 (5) (2000) 2232.
[9] D. Kaganovich, A. Ting, C.I. Moore, A. Zigler et al., Phys. Rev. E 59 (5) (1999) R4769.
[10] J.P. Verboncoeur, A.B. Langdon, N.T. Gladd, Comput. Phys. Commun. 87 (1995) 199, codes available via http://ptsg.eecs.berkeley.edu.
[11] P. Mardahl, J.S. Wurtele, P. Mardahl Ph.D. Thesis, Department of Electrical Engineering and Computer Science, University of California, Berkeley, 2001.
[12] G. Shvets, N.J. Fisch, A. Pukhov, J. Meyer-ter-Vehn, Phys. Rev. Lett. 81 (22) (1998) 4879.
[13] H.J. Lee, P. Mardahl, G. Penn, J. Wurtele, IEEE Trans. Plasma Sci. (Special Issue) (2002), submitted for publication.